AN AEROSOL OPTICAL DEPTH PRODUCT FOR NOAA'S SURFRAD NETWORK

John A. Augustine*, Joseph J. Michalsky, and Gary B. Hodges
NOAA Earth System Research Laboratory
Global Monitoring Division
Boulder, Colorado

1. INTRODUCTION

SURFRAD is the first national surface radiation budget network for the United States (Augustine et al. 2000; Augustine et al. 2005). It currently has seven stations that sample the surface radiation budget in various climate types of the U.S. (Fig. 1). The network became operational in 1995 with four stations. Penn State and Desert Rock were added in 1998, and the latest station at Sioux Falls, SD was installed in 2003. To fulfill its role as a research network, in addition to the basic surface radiation budget, several ancillary observations and calculations are made. These include sky cover measurements, interpolated National Weather Service-type soundings to each station, a clear-sky identification product, and spectral solar measurements. This paper reports on the series of algorithms that was developed to process the spectral solar measurements for aerosol optical

Figure 1. NOAA's Surface Radiation Budget Network—SURFRAD.

_____

Corresponding author address: John A. Augustine, NOAA/ESRL/GMD, R/GMD2, 325 Broadway, Boulder, CO 80305; e-mail: John.A.Augustine@noaa.gov.

depth (AOD). The method takes advantage of SURFRAD products, measurements, and novel automated tasks that make this traditionally arduous procedure more efficient, and the AODs more accurate.

2. The MFRSR

The MultiFilter Rotating Shadowband Radiometer (MFRSR) is used at SURFRAD stations for spectral solar measurements. Channels of the MFRSR are 10 nm wide and peak nominally at 415, 500, 614, 670, 868, and 940 nm. It also has a broadband solar channel. The MFRSR is a sunphotometer that infers the solar beam intensity for its various channels by making successive global and diffuse measurements and computing their difference. A carefully documented cosine response is applied, ensuring that the computed beam intensity at large solar zenith angles is accurate. Samples are made at 15-second intervals and two-minute averages of the global, diffuse, and inferred spectral beam intensities are recorded for all channels. Because the MFRSR operates continuously, its data stream includes all weather types. Both the channel calibration and AOD calculation processes require clear views of the sun, therefore a large part of the automation of these procedures involves screening for appropriate data.

3. Calibration of MFRSR channels

Both the calibration procedure and aerosol optical depth calculation use the Beer-Lambert equation:

$$V = V_o e^{-m \Sigma \tau} \qquad (1)$$

where V is the inferred beam voltage for a particular channel, V_o is the beam voltage that the instrument would sense above the atmosphere, m is the path length of the solar beam through the atmosphere at the time of the measurement, and $\Sigma \tau$ is the total extinction by all

atmospheric constituents along that path that affect the wavelength being measured. $\Sigma\tau$ is also called the "total optical depth." Equation (1) is linearized by taking the log of both sides:

$$\ln(V) = -m\Sigma\tau + \ln(V_o) \qquad (2)$$

A plot of the natural log of the inferred direct beam voltage vs. the solar beam path length for various times of an optically clear morning or afternoon would result in a straight line, as in Fig. 2. Such diagrams are referred to as calibration Langley plots (Shaw 1983). The slope of a Langley plot is the total optical depth of the atmosphere, and the extrapolated y-intercept, $\ln(V_o)$, which represents a path length of zero, is the inferred voltage of the beam measurement above the atmosphere. $\ln(V_o)$ from a calibration Langley plot is a reference for the instrument because it is virtually constant and should only be affected by cyclical changes in the earth-sun distance. That value, combined with any MFRSR measurement made within a few weeks of the day that the reference point was set, on the same type of plot as Fig. 2, would yield a total optical depth for the time of the measurement. A benefit of this calibration procedure is that the absolute calibration of the MFRSR channels is not necessary.
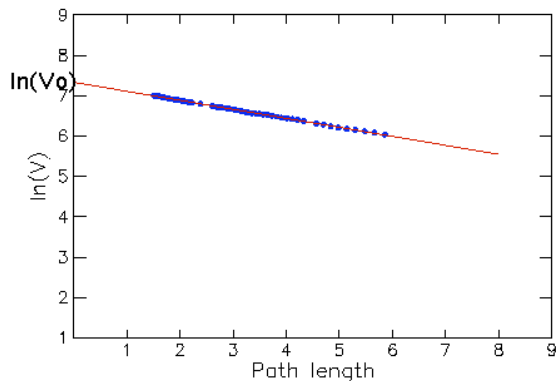
Figure 2. Example of a calibration Langley plot. Blue points represent the natural log of inferred MFRSR beam voltages for times when the instrument measured an unobscured solar beam.

MFRSRs operate continuously and produce a large amount of data--much of it unsuitable for this type of application. To manually choose acceptable periods for calibration from the continuous MFRSR data stream is tedious, and especially difficult to automate. Augustine et al. (2003) introduced a method whereby periods identified as totally cloud free by the Long and Ackerman (2000) clear-sky identification method are used to screen MFRSR data. If the sky is cloud free, then the sun's beam is expected to be unobscured, and those times should be suitable for calibration Langley plots. Periods for calibration Langley plots are identified in the MFRSR data stream by cross referencing the continuous MFRSR data with times detected as clear in the SURFRAD clear-sky product. The clear-sky algorithm will erroneously dismiss periods with high aerosol content, even though the sky may be clear, because it relies on the diffuse measurement being low. Although that is a detriment to clear sky detection, it benefits its use here because only the cleanest and brightest skies are used to identify calibration data. In this algorithm, calibration Langley plots are restricted to measurements between 1.5 and 6 atmospheres, following arguments made in Michalsky et al. (2001)

The calibration method developed for SURFRAD MFRSRs is run for sequential one- or two-month segments over the tenure of a particular MFRSR. The length of the period sampled depends on the number of Langley plots identified within that period. A representative V_o for the period processed is defined as the average of that sample. The results for May and June 2005 for the 500-nm channel of the Table Mountain MFRSR are shown in Fig. 3. Figure 3 contains 16 Langley plots that were chosen automatically over the two-month period. The blue points represent the times of clear sky. Only those points were used for the linear fits (red lines). Notice that the extrapolations of the Langley plots converge at the y-axis. This convergence is expected because the intercept represents the extraterrestrial value, or solar constant, for that channel's wavelength. However, note that in Fig. 3 there is a spread in the intercept values. Theoretically, the variation in the V_o's should not be as great as that shown because only the annual oscillation in the earth-sun distance should affect the solar constant. To remove that known variation from the sample, the extrapolated V_o's are normalized to a circular earth orbit before averaging. These corrected intercepts are referred to as V_o^*. However, a spread in the sample of corrected intercepts remains because some of the automatically

derived Langley plots probably represent non-optimum conditions that likely would have been rejected if this procedure were done manually. For example, variations in aerosol loading over the time of a Langley plot will cause a slightly curved plot that will not extrapolate well. Notice the curvature in the plotted blue dots of the lowest Langley plot in Fig. 3. To solve this problem, outlier V_o^* values are removed from the sample by statistical methods. In an initial screening, all V_o^* values more that one standard deviation from the sample mean are rejected. Then all V_o^* values greater than 1.5 standard deviations from the remaining sample are rejected. Last, large deviations from the linear fits of the remaining Langley plots are screened out, and the remaining points are re-fit by linear least squares regression. The result is a tighter grouping of Langley plots and ultimately, less variation in the final sample (Fig. 4). Of the 16 Langley plots in Fig. 3, 11 V_o^* values survived the outlier elimination procedure. The mean V_o^* from the reduced sample is considered to be the representative calibration for the two-month period, and the scatter in the reduced V_o^* sample defines the error. A standard propagation of error method reported in Michalsky et al. (2001) is used to compute the error. This calibration procedure is carried out for the first five spectral channels of the MFRSR. The 940-nm channel is not processed because it is overwhelmed by water vapor absorption.

To ensure smoothly varying channel calibrations, the "representative" mean Langley calibrations covering one- or two-month periods are analyzed in time series over multi-year periods (Fig. 5). These time series are fit to functions so that daily calibration values can be identified for aerosol optical depth calculations. Because MFRSR channel sensitivities drift slowly, linear fits to the multi-year time series were attempted (dotted lines in Fig. 5). However, a slight intra-annual periodicity in the orbit-normalized calibrations consistently appeared for all MFRSRs, at all stations, and for all channels. Mean summer V_o^*'s are consistently higher in magnitude than
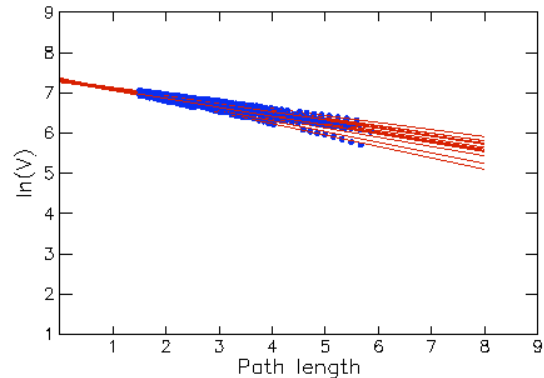
Figure 3. Composite of 16 Langley plots for May and June 2005 for the 500-nm channel of the Table Mountain SURFRAD MFRSR.
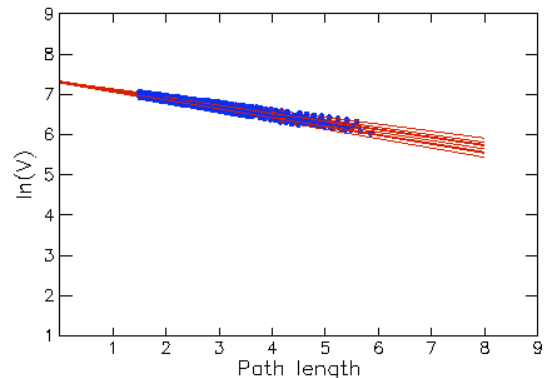
Figure 4. As in Fig. 3, but after five Langley plots responsible for outlier V_o values were removed.

those in winter. We concluded that this regular and repeatable variability is a consequence of the MFRSR's sensitivity to the ambient temperature. Therefore, a periodic function with sine and cosine terms, and a linear term to account for sensitivity drift, was fit to each time series (solid curves in Fig. 5). The time series of error associated with the representative Langley calibrations did not show the same intra-annual periodicity and therefore the errors were fit to a linear expression (not shown). Before the fits are computed, the multi-year time series are overlapped by four months on either end to ensure smooth transitions of the calibration and error expressions between successive two-year periods.
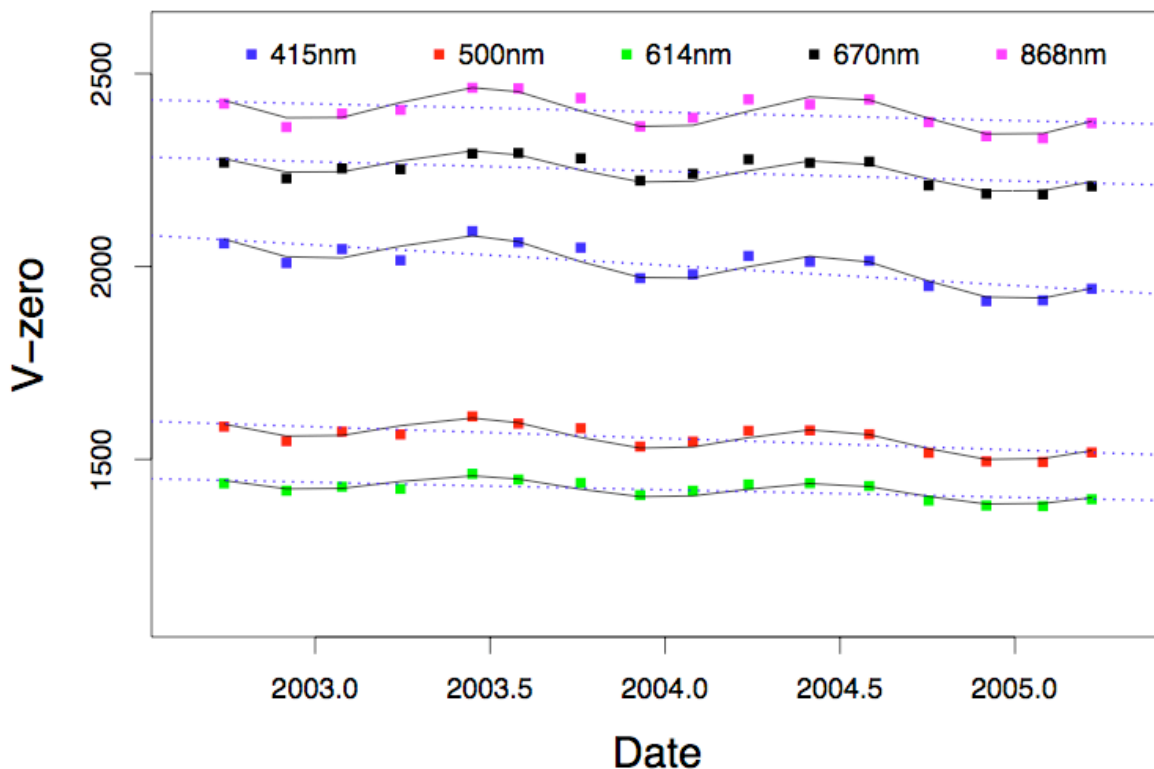
Figure 5. Time series of orbit-normalized V_o two-month means (squares) for five channels of the Table Mountain MFRSR for 2003 and 2004. The curved lines are Fourier fits to the time series, and the dotted lines are linear fits.

4. Aerosol optical depth calculation

The first step in the AOD calculation is the retrieval of channel-specific orbit-normalized calibrations, V_o^*, for the day being processed using the best-fit periodic equations that describe their variations over the tenure of the instrument. Retrieved V_o^* calibrations are then corrected to the appropriate earth-sun distance for the day being processed. The resultant day-specific V_o, along with each MFRSR measurement of that day are then applied to the Beer-Lambert law to compute a daily time series of *total optical depth* for each channel. *Aerosol optical depth* is computed by subtracting the contributions of molecular scattering and ozone absorption specific to each channel from the total optical depth. Ozone absorption coefficients are chosen based on the central wavelengths specific to channels of the MFRSR that made the measurements. A daily value of total ozone for the date being processed is automatically obtained from a NASA/TOMS web site for the specific location of the station. Molecular scattering is accurately computed for each channel using the station pressure measured at the SURFRAD station at the time of each MFRSR measurement. Contributions to the total optical depth by nitrogen dioxide absorption are negligible for all channels but 415-nm. Therefore the aerosol optical depths computed for the 415-nm channel may be erroneously high on high pollution days.

The final step is to subject each daily time series of AOD to cloud screening because AOD can only be computed for times that the sun's beam is cleanly sensed by the MFRSR. Initially, all AODs greater than 2.0 are discarded, which eliminates MFRSR measurements made in the presence of thick clouds. The remaining values are subject to a temporal stability test. The basis for that test is that when the solar beam passes through thin clouds, the measured MFRSR signals are more variable relative to the more stable cloud-free signals that are only affected by aerosols.

An example of the 500-nm AOD time series for 17 April 2001 at Table Mountain is shown in Fig. 6. This day was in the midst of an Asian dust outbreak over the U.S., thus the values of AOD are rather high. The blue points

represent AOD values that passed the cloud screening and are labeled with a good quality control mark in the daily product file. The red points did not pass the screening test, and because of that failure we are not confident that they solely represent aerosol extinction. The large scatter in the red points earlier in the day is definitely caused by clouds. The red points clustered near, or at the same level of the blue points had enough variation to be rejected by the cloud-screening algorithm, but some of those may have been wrongly excluded. Errors in the AODs are shown as gray dots in Fig. 6. The AOD errors vary systematically with solar zenith angle; the smaller the solar zenith angle, the larger the error. Note in Fig. 6 that for 1200 LST, the time when the solar beam path length is smallest, the error bars are largest.
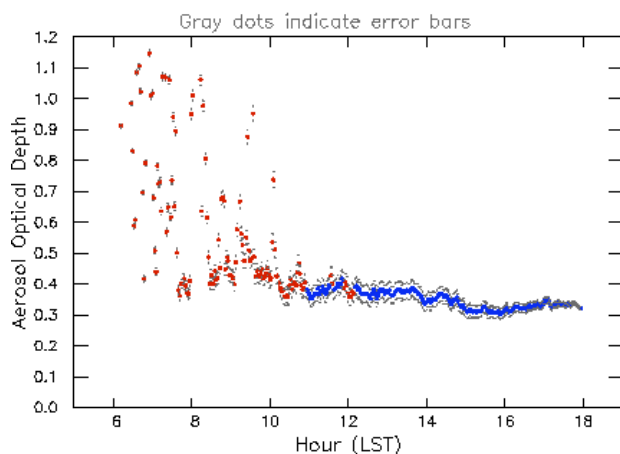
Figure 6. Time series of AOD for the 500-nm channel for 17 April 2001 at the Table Mountain, Colorado SURFRAD station. Blue points are times that passed the cloud-screening test, and thus represent believable AOD values. Red points did not pass the cloud screening, and the gray dots are error bars.

5.   Results

The complete algorithm was run on the Table Mountain MFRSR data record from 1997 through 2005. Daily averages of 500-nm AOD are plotted in time series over that nine-year period in Fig. 7. An annual periodicity of high AOD in summer and low values in winter is readily apparent, although there appears to be a pronounced inter-annual variability. Some years, such as 1998, 2001, 2002, and 2003, have higher AODs than the other years. The largest values of the time series in the summer of 2002 were caused by forest fires that were pervasive that year owing to a prolonged drought.

To get a sense of the typical annual cycle of AOD for Table Mountain, the nine years of data in Fig. 7 were compiled into a mean annual time series of monthly means. That summary is shown in Fig. 8 for all channels. When plotted in that mode, the repeatable seasonal signals emerge. The most obvious are the summer maximum and winter minimum. Another prominent feature is the relative maximum in March and April that is caused by the yearly intrusion of Asian dust.

Multi-spectral analyses of AOD in this manner can yield information concerning the relative particle size of the aerosols through the Angstrom exponent. The Angstrom exponent is the absolute value of the slope when plotting the natural log of the AOD computed for two or more channels versus the natural log of those channels' wavelengths. The resultant slope is inversely proportional to the mean size of the aerosol particles. An Angstrom exponent of 0 indicates very large particles, and a value of 4 is representative of molecules. Continental aerosols typically have an Angstrom exponent of about 1.3. The Angstrom exponent computed for July in Fig. 8 is 1.52, and that for April, when Asian dust is usually present in Colorado, is 0.98. These values are reasonable and indicate that in the summertime, when aerosols are dominated by smoke and photochemistry, particles are relatively small. In the spring, local aerosols are typically combined with imported Asian dust, and are relatively large.
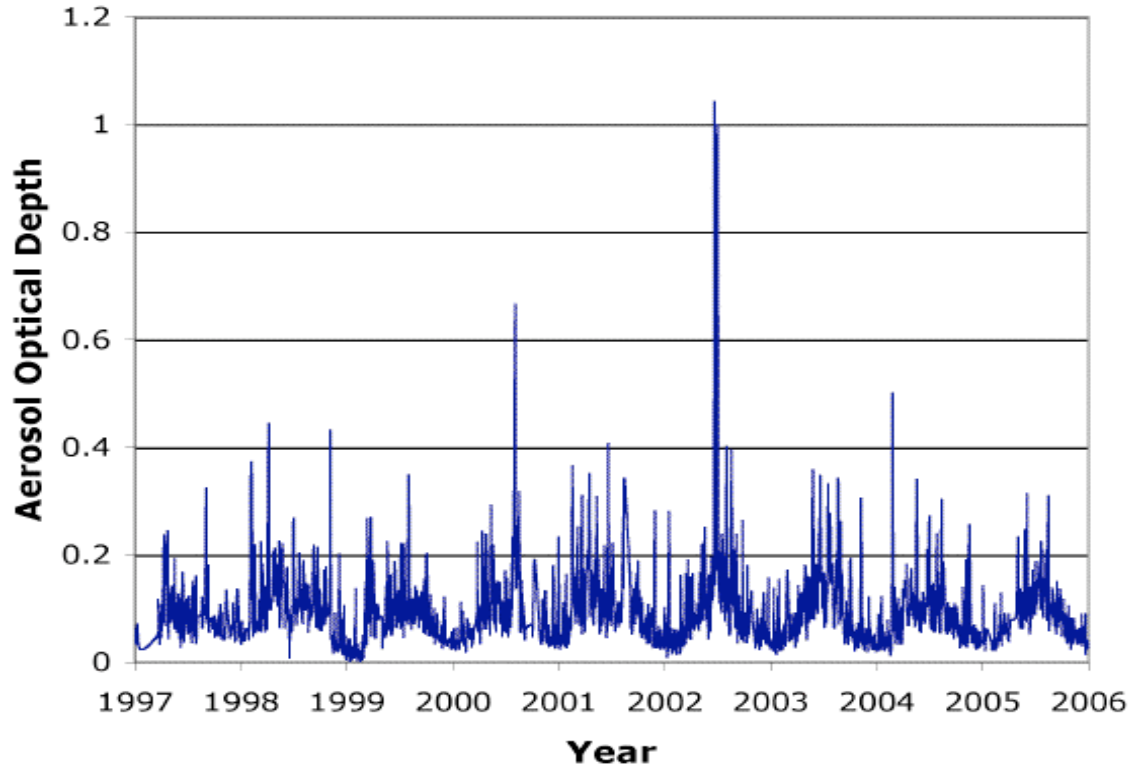
Figure 7. Long-term time series of 500-nm AOD daily averages for the Table Mountain, Colorado SURFRAD station.
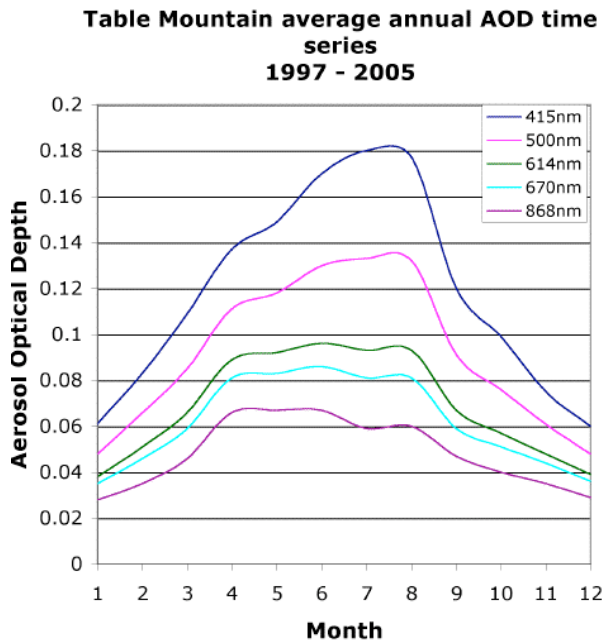
Figure 8. Mean annual time series aerosol optical depth for the Table Mountain SURFRAD station (1997-2005), for the five spectral channels of the MFRSR.

6.   Summary

The MFRSR calibration and AOD analysis algorithms developed for the SURFRAD network include several unique features that minimize error and facilitate these complicated procedures. The once painstaking task of identifying calibration Langley plots is uniquely automated by cross-referencing the MFRSR measurements with the SURFRAD clear-sky product. Use of the clear-sky product ensures that measurements used for Langley calibrations are not compromised by clouds and represent relatively clean conditions. Identifying mean channel-specific Langley calibrations that represent one- or two-month periods and grouping them in time series over two-year periods allows for the resolution and removal of the temperature dependence of the MFRSR, thus further reducing error in the ultimate product. Finally, the use of measured SURFRAD station pressure for accurate molecular scattering calculations at the resolution of the measurements, and the automatic acquisition of daily total ozone over each station for spectral ozone absorption

calculations further improve the accuracy of the SURFRAD AOD calculation. The first test of this new algorithm on nine years of Table Mountain MFRSR data yielded good results. Provisional AOD data for SURFRAD stations can now be computed. However, before a final product can be released, the central wavelengths of the MFRSRs that have been used at SURFRAD stations must be checked and verified.

7. References

Augustine, J. A., C. R. Cornwall, G. B. Hodges, C. N. Long, C. I. Medina, and J. J. DeLuisi, 2003: An automated method of MFRSR calibration for aerosol optical depth analysis with application to an Asian dust outbreak over the United States, *J. Appl. Meteor.*, **42**, 266-278.

Augustine, J. A., J. J. DeLuisi, and C. N. Long, 2000: SURFRAD—A national surface radiation budget network for atmospheric research. *Bull. Amer. Meteor. Soc.* **81**, 2341-2357.

Augustine, J. A., G. B. Hodges, C. R. Cornwall, J. J. Michalsky, and C. I. Medina, 2005: An update on SURFRAD—The GCOS surface radiation budget network for the continental United States, *J. Atmos. And Oceanic Tech.*, **22**, 1460–1472.

Long, C. N. and T. P. Ackerman, 2000: Identification of clear skies from broadband pyranometer measurements and calculation of downwelling shortwave cloud effects. *J. Geophys. Res.*, **105**, D12, 15609-15626.

Michalsky, J. J., J. A. Schlemmer, W.E. Berkheiser, J.L. Berndt, L.C. Harrison, N.S.Laulainen, N.R. Larson, and J.C. Barnard, 2001: Multiyear measurements of aerosol optical depth in the Atmospheric Radiation Measurement and Quantitative Links programs, *J. Geophys. Res.*, **106**, (D11), 12099-12107.

Shaw, G. E., 1983: Sun photometry. *Bull. Amer. Meteor. Soc.,* **64**, 4-10.